Study of ferromagnetic instability in τ-MnAl, using first-principles

Kanika Anand, J.J. Pulikkotil, S. Auluck *

National Physical Laboratory, Council of Scientific & Industrial Research, Dr. K.S. Krishnan Marg, New Delhi 110012, India

A B S T R A C T

The τ- phase of the binary Mn-Al system is a promising rare-earth free permanent magnet. However, the experimentally determined figure-of-merit (energy-factor) is significantly lower than the theoretical estimate. This is partly being associated with the low volume fraction of τ-MnAl during synthesis, chemical disorder driven inter-sublattice antiferromagnetism, and presence of multiple binary phases. In this work, with the help of first-principles linear response calculations, we show that the presumed long range ferromagnetic ordering in τ-MnAl is unstable. Calculation of Mn magnetic pair-exchange interaction for τ-MnAl show competing ferromagnetic and antiferromagnetic interactions. As a result, the study infers to a non-collinear magnetic ground state, which then partly explains the low magnetization as observed in experiments. Local probe experiments such as neutron diffraction, corroborating our prediction of the non-collinear state in τ-MnAl is therefore desired.

© 2014 Elsevier B.V. All rights reserved.

1. Introduction

With increasing demand of permanent magnets based technology and limited global supply of rare-earths, the need for rare-earth free magnets has received widespread attention. Based on the material pre-requisites, sampling permanent magnets have been largely focused around conventional ferromagnets, which have high magnetization and Curie temperature. Among these class of materials, AlNiCo, ferrites, binary Pt–Co alloys and others have been found to be promising materials [1–6]. High magnetic anisotropy as well as magnetization is also reported in Mn based binary alloy systems such as Mn–Bi [7–11], Mn–Ga [12–16] and Mn–Al [17,19,18]. However, unlike MnAl, the commercial acceptance of Mn–Bi and Mn–Ga alloys are limited due to their quick degradation and/or little abundance of the Ga and Bi constituents. Beyond, abundance and global distribution of Mn and Al resources in the earth's crust and its eco-friendliness make MnAl alloys a promising material among the rare-earth free permanent magnets.

In its tetragonal phase (the τ-phase) MnAl is reported to be conventional ferromagnetic (FM) material with relatively high saturation magnetization ($2.4\,\mu_B$/Mn) and high magneto-crystalline anisotropy energy (0.259 meV/f.u). The theoretical estimate of its energy product ($\simeq 12$ MG Oe) [20] is comparable with that of the widely used and expensive AlNiCo alloys. However, experiments find a much lower value ($\simeq 5$ MG Oe) [19–23]. The reduction has been largely associated with low saturation magnetization which

is mainly attributed to the antiferromagnetic (AFM) interactions in the system [24].

The general chemical representation of τ-MnAl is $Mn_{0.5+\delta}Al_{0.5-\delta}$; $0 < \delta \leq 0.15$, with an underlying tetragonal crystal structure of p4/mmm symmetry (space group no. 123). For the hypothetical stoichiometric compound, referring to the case $\delta = 0$, the Mn and Al ions are at the $(0,0,0)$ and $(0,0,\frac{1}{2})$, which are designated as the 1(a) and 1(b) Wyckoff positions of the unit-cell, respectively. The τ-phase is chemically disordered with extra Mn ions substituting the Al ions at the 1(b) sites. These Mn ions in the Al sublattice interact antiferromagnetically with the Mn ions at the 1(a) site, leading to a reduction in the net magnetization of the material. Besides, low volume fraction of the τ-phase during synthesis, co-existence of multiple binary Mn-Al phases, un-reacted Mn and defects have also been attributed to the observed low magnetization in τ-MnAl [19,24–31].

Apart from the factors that mentioned above, which lead to low magnetization in τ-MnAl, our linear response calculations, based on density functional theory, indicate an instability of a long range collinear FM ordering of the Mn moments. The calculations estimating the Mn magnetic pair-exchange interactions reveal competing FM and AFM interactions in τ-MnAl. This is in contrast with the earlier reports, which presumed a collinear FM structure as the equilibrium state for τ-MnAl. Therefore, what follows from our calculations might be considered as a strong evidence of a non-collinear magnetic ground state for τ-MnAl, which normally evolves due to competing FM and AFM interactions [32], and therefore requires experimental corroboration. Also, we find that the nature of Mn magnetic moments at the 1(a) and 1(b)

* Corresponding author.
  E-mail addresses: sauluck@gmail.com, sauluck@iitk.ac.in (S. Auluck).

crystallographic sites of the non-stoichiometric τ-MnAl are remarkably very different. Volume dependence study of Mn local moments reveals that the Mn magnetic moments at the 1(a) and 1(b) sites have itinerant and localized nature, respectively.

2. Computational details

The structural and magnetic properties of τ-MnAl are studied using the ab-initio density functional based Korringa-Kohn-Rostoker (KKR) method formulated in the atomic-sphere approximation (ASA) [33] including the use of muffin-tin correction for the Madelung energy and the multi-pole moment correction to the Madelung potential and energy [34]. The partial waves are expanded up to $l_{max} = 3$ inside the atomic spheres. The chemical and magnetic moment disorder are taken into account by means of coherent potential approximation (CPA) [35]. The local density approximation (LDA) were considered to describe the exchange-correlation effects of the crystal Hamiltonian. The atomic sphere radii of Mn and Al were kept the same, which result in a overlap volume of $\simeq 12\%$, legitimately within the accuracy of the approximation. The number of k- points for determining the total energies were kept in excess of 2600 k-points, corresponding to a Monhorst-Pack grid of $36 \times 36 \times 28$, in the irreducible wedge of the Brillouin zone. The lattice constants of τ-MnAl was taken from the experiments, *i.e.*, $a = 2.73$ Å and $\frac{c}{a} = 1.298$.

3. Results and discussion

3.1. Energetics

First, we consider the hypothetical stoichiometric system τ-Mn$_{0.50}$Al$_{0.50}$. Assuming that the magnetic ordering is collinear, we performed few calculations considering the FM and certain AFM ordering of the Mn ions positioned at the 1(a) site of the unit-cell. Comparing the total energies we find that the FM ordering of Mn spins has the lowest energy, among the various collinear structures considered. The total energy of the A-type AFM ordering was determined to be 50.88 meV/f.u higher in comparison with the FM structure, while for the C- and G-type AFM ordering the corresponding values were 84.86 and 202.08 meV/f.u, higher. Note that the nomenclature we follow to describe the AFM structures are that from the works of Wollan and Koehler [36].

To model the τ-phase, which is disordered and non-stoichiometric (τ-Mn$_{0.54}$Al$_{0.46}$), we employ CPA. Total energy calculations find that the minimum corresponds to a FM ordering of the Mn ions at the 1(a) sites, with Mn in the 1(b) being antiferromagnetically coupled to the Mn ions at the 1(a) sub-lattice. We also note that the AFM interaction is robust between the 1(a) and 1(b) sub-lattice, since the calculations always converged to such an AFM ordering irrespective of the initial magnetic ordering assigned in the calculations. This was also verified against the computational parameters such as atomic sphere radii of the ions and the k-mesh grid. The results are consistent with the predictions of Sakuma [24], who has attributed the observed low magnetization in τ-Mn$_{0.54}$Al$_{0.46}$ to AFM emanating from the excess of Mn ions in the Al sub-lattice.

We have also computed the energy difference between the FM structure and the disordered local moment (DLM) structure. In the DLM method, an uniform probability is assigned to the magnetic moments to orient in all possible directions, resulting in no net magnetization. In this scenario, DLM mimics a paramagnetic state, the energy difference of which with respect to the equilibrium ordered structure would then provide a reasonable estimate to the magnetic transition temperature (T_c). Our KKR-CPA method, find the difference in the total energy of the ground state magnetic structure with that of the DLM (paramagnetic) structure as 48.9 meV/atom ($\simeq$567 K), which is comparable with the experimentally measured T_c of 650 K.

3.2. Electronic structure

The density of states of the hypothetical stoichiometric MnAl system has been reported earlier [20,24,37]. Our results with the KKR-ASA method are consistent with the earlier reports and is

shown in Fig. 1. For the stoichiometric MnAl, the Al and Mn states are wide spread over the entire energy range, depicting the covalent nature of bonding in the system. The Fermi energy is positioned in a valley like feature for both majority and minority bands, suggesting an electronic stability [24].

In Fig. 1, we compare the total and sub-lattice resolved partial Mn 3d- density of states of τ-Mn$_{0.54}$Al$_{0.46}$. Substitution of Mn at the Al site, in the τ-phase structure preserves the overall features of the band structure. The Mn states at the 1(b) sites are hybridized with the Al derived sp states. The covalent bonding characteristics of the material appears unaltered with the addition of Mn ions in the Al-sub-lattice. The states that constitute the Fermi energy are primarily composed of the 3d states, originating from the Mn ions located at the 1(a) and 1(b) sites. The extra Mn ions also does not alter the position of the Fermi energy in comparison with the stoichiometric MnAl system. We note that Fermi energy cuts both majority and minority spin bands in τ-Mn$_{0.54}$Al$_{0.46}$. This classify τ-MnAl as a weak FM system. The total density of states of the majority and minority spin bands at Fermi energy is 0.22 and 0.52 St./eV-atom, which are mainly Mn 3d in character.

3.3. Magnetism and exchange interactions

The calculated Mn local magnetic moments in τ-Mn$_{0.54}$Al$_{0.46}$ at the 1(a) and 1(b) sites are 2.41 and -2.99 μ_B, respectively. This yields the net magnetization (concentration weighted) to be 2.10 μ_B/cell, accounting the small negative polarization of -0.08 μ_B at the Al sites. For the stoichiometric material MnAl, the Mn local moment is determined to be 2.42 μ_B. Thus, consistent with the prediction of Sakuma, we find that excess of Mn in the Al sub-lattice reduce the magnetization of the τ-phase [24]. However, the theoretical magnetization value for the disordered τ-Mn$_{0.54}$Al$_{0.46}$ is still higher than the experimental value of $\simeq$1.5 μ_B [38–40]. Further, considering the τ-phase with composition Mn$_{0.57}$Al$_{0.43}$, the local moments on Mn at the 1(a) and 1(b) sites were determined as 2.40 and -2.98 μ_B, with net magnetization of 1.92 μ_B. It is interesting to note that the magnitude of the Mn local moments at the 1(a) and 1(b) sites remains more or less invariant with respect to chemical disorder in the system. However, the net magnetization of the system decreases with increasing Mn/Al
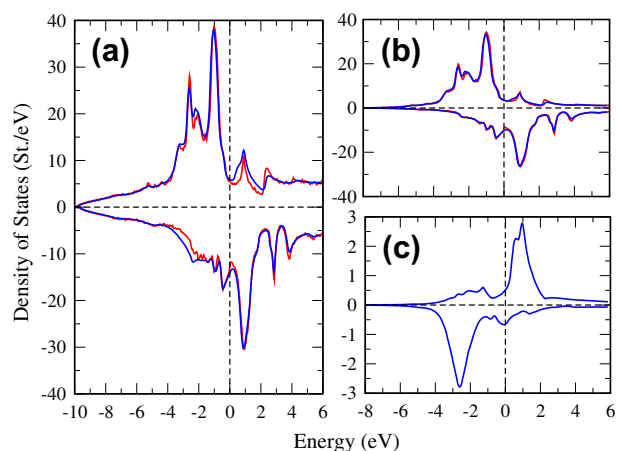

Fig. 1. Comparison of the spin polarized density of states of the stoichiometric MnAl (red curves) and Mn$_{0.5+\delta}$Al$_{0.5-\delta}$; $\delta = 0.04$ (blue curves) calculated using the KKR-ASA-CPA method. Panel (a) the total density of states expressed in eV/f.u. Panels (b) represents the 3d partial density of states of Mn at the 1(a), while panel (c) shows the concentration weighted 3d partial density of states of Mn at the 1(b) site. Note that the Mn at the 1(a) and 1(b) crystallographic site of the P$_4$/mmm (space group: 123) unit cell symmetry are antiferromagnetically coupled. The vertical line through energy zero represents the reference Fermi energy. (For interpretation of the references to color in this figure legend, the reader is referred to the web version of this article.)

disorder due to the AFM coupling of the inter-sublattice Mn ions. Therefore, for the optimization of the permanent magnet characteristics, where high magnetization is a per-requisite, the concentration of Mn ions in the Al sub-lattice must be minimized.

We also study the volume dependence of the Mn magnetic moment in the τ-phase for the composition τ-$Mn_{0.54}Al_{0.46}$. The results are shown in Fig. 2. In the ferromagnetically ordered structure, we find that the magnetic moment of the Mn ions at both 1(a) and 1(b) sites increases (decreases) with increasing (decreasing) cell volume. For a relative decrease in volume by $\simeq 25\%$, the magnetization decreases from 2.1 μ_B at its equilibrium to 1.5 μ_B. Thus, we find that both increase in the Mn concentration in the τ-phase as well as decrease in volume, reduces the net magnetization of the material.

Solution to a DLM state, often serve as a good indicator to propose the nature of magnetism in a given system, i.e., whether the magnetic moments are localized or itinerant. The DLM calculations, in general, yield a local magnetic moment solution for localized magnets, but not for itinerant ones. Volume dependence of the magnitude of the Mn disordered local moment at the crystallographic 1(a) and 1(b) sites are shown in Fig. 2(b). We find that the DLM state ceases to exist for compressed volumes. However, with increasing cell volume the magnitude of the Mn local moments at 1(a) and 1(b) sites tends to be similar in magnitude. This infers to change in the magnetism properties in τ-$Mn_{0.54}Al_{0.46}$ material with volume. The excess Mn substituted in the Al sub-lattice shows a transition from itinerant character at compressed volumes to localized at expanded volumes. However, the Mn at the 1(a) sites depicts a local moment characteristics at all volumes considered, although there is a steady reduction in its magnitude upon compression of the unit cell.

Till date, the τ-phase is the only reported FM phase in the entire Mn-Al binary phase diagram. For all other binary phases, either some form of AFM or non-collinear structures as their ground state [41,42]. Within the collinear models, finding that the lower energy state in τ-MnAl is FM, we calculated the magnetic pair exchange parameters, $J_{ij}(\overrightarrow{R})$ to check for its magnetic stability. The pair exchange interaction parameters were calculated in the mean field approximation as described in Ref. [43,44]. In this linear response technique, the energies of small deviations from the reference state (here in this case, the FM state) is mapped on to the Heisenberg model, $\Delta E = \sum_{i,j} J_{ij} S_i S_j$.
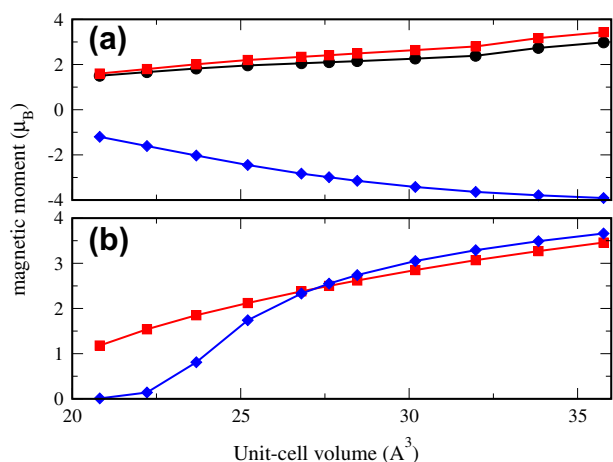

Fig. 2. The volume dependence (with constant $\frac{c}{a}$, =1.298) of Mn local magnetic moments in τ-$Mn_{0.54}Al_{0.46}$. The upper panels corresponds to the the FM structure (see text), and lower panel to the corresponding DLM structure. Filled black circles represented the net magnetization in the unit-cell for the FM ordering while the red squares and blue diamonds represent the local magnetic moments of the Mn ions at the 1(a) and 1(b) sites of the tetragonal unit cell. The equilibrium volume is 27.623 Å^3. (For interpretation of the references to color in this figure legend, the reader is referred to the web version of this article.)

In Table 1 we present the magnetic pair-exchange parameters $J_{\overrightarrow{R}}$ for τ-$Mn_{0.54}Al_{0.46}$, at the equilibrium volume. It is interesting to note that the magnitude of the first near neighbor AFM interaction (0.612 meV) between Mn atoms in 1(a) sub-lattice and 1(b) sites, along the connecting vector $\overrightarrow{R} = (\frac{1}{2}, \frac{1}{2}, \frac{1}{2})$ is comparable to that of the second near neighbor FM interaction with $\overrightarrow{R} = (1, 0, 0)$, i.e., 0.601 meV. Similar is the case with J_5 and J_6, where the FM and AFM interactions between the Mn spins have similar magnitudes. Besides, calculations also find instability (negative) of the FM interaction along $\overrightarrow{R} = (1, 0, 1)$. In the most commonly accepted theories, emergence of non-collinear magnetic ordering is either associated with magnetic frustration induced by crystal geometry with AFM exchange interactions or due to the presence of competing near neighbor FM and AFM interactions [45,46]. Thus, for the case of τ-$Mn_{0.54}Al_{0.46}$ the existence of competing FM and AFM interactions are suggestive of a non-collinear ordering of Mn moments.

To understand whether the few extra at% of Mn in the τ-$Mn_{0.54}Al_{0.46}$ have any significant role in modifying the inter-atomic interactions among the Mn ions at the 1a sites, we perform calculations for the stoichiometrically ordered $Mn_{0.5}Al_{0.5}$ system, assuming the same crystal parameters like that of the τ-phase. For this hypothetical $Mn_{0.5}Al_{0.5}$ system, we find the magnitudes of J_2, J_3, J_4 and J_5 to be 0.973, 1.234, 0.961 and -0.733 meV, respectively. Thus, it becomes evident that the ferromagnetic instability in τ-$Mn_{0.54}Al_{0.46}$ is mainly introduced by the extra Mn ions in the Al sub-lattice. Besides, we also find that the strength of the ferromagnetic exchange interaction between the Mn ions in the 1a sub-lattice is also decreased. For instance, the value of J_2 in $Mn_{0.5}Al_{0.5}$ decreases by $\simeq 35\%$ with an addition of 0.04 at% of Mn in the Al sub-lattice.

In order to study the stability of the FM structure of τ-$Mn_{0.54}Al_{0.46}$ as a function of cell volume, we calculated the Mn-Mn pair exchanges, $J_{\overrightarrow{R}}$ with c/a ratio held fixed to the experimental value (=1.298). These pair-exchange parameters are indexed by the crystallographic indices of the connecting $\overrightarrow{R}$ of the tetragonal structure, details of which are illustrated in Table 1. The results of the variation in the $J_{\overrightarrow{R}}$ with respect to $\Delta a/a_0$ (in %), where $a_0 = 2.73$ Å and $\Delta a = (a - a_0)$ are shown in Fig. 3. The most striking feature is the change in sign of $J_{\overrightarrow{R}}$ for those corresponding to $\overrightarrow{R} = (\frac{1}{2}, \frac{1}{2}, \frac{1}{2})$ and $\overrightarrow{R} = (1, 0, 0)$ with increasing cell volumes. While $J_1 \left(\overrightarrow{R} = (\frac{1}{2}, \frac{1}{2}, \frac{1}{2}) \right)$ changes sign showing instability of the AFM ordering at $\simeq +3\%$ increase in cell volume, J_2 $\left(\overrightarrow{R} = (1, 0, 0) \right)$ reverses its sign at $\simeq 1.5\%$ showing FM instability among the Mn spins in the tetragonal basal plane. Besides, it is also deduced that there exists competing magnetic interactions leading

Table 1
The first seven Mn–Mn ($J_{\overrightarrow{R}}$) pair-exchange parameters in τ-$Mn_{0.54}Al_{0.46}$ with lattice constants $a = 2.771$ and $c = 3.597$ Å. Column "n" denotes the number of equivalent nearest neighbors together with the spin orientation, $\overrightarrow{R}$ the vector connecting the central Mn ion to neighboring Mn ions in units of the lattice parameter and $|R|$ for the distance to the central atom. $J_{\overrightarrow{R}}$ is related to the Heisenberg model $J_{\overrightarrow{R}}^H$ as $J_{\overrightarrow{R}} = J_{\overrightarrow{R}}^H S S_j$.

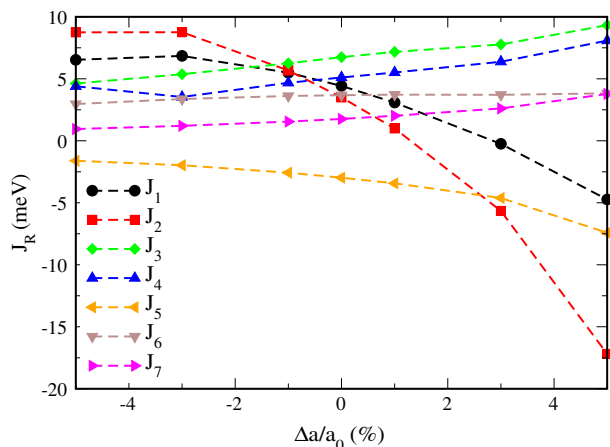|	n	$\overrightarrow{R}$	$|R|$ (Å)	$J_{\overrightarrow{R}}$ (meV)	$J_{\overrightarrow{R}}^H$ (meV)
J_1	8 (↓)	$(\frac{1}{2}, \frac{1}{2}, \frac{1}{2})$	2.659	4.423	-0.612
J_2	4 (↑)	$(1, 0, 0)$	2.771	3.498	0.601
J_3	2 (↑)	$(0, 0, 1)$	3.597	6.746	1.158
J_4	4 (↑)	$(1, 1, 0)$	3.919	5.107	0.877
J_5	8 (↑)	$(1, 0, 1)$	4.541	-2.978	-0.511
J_6	16 (↓)	$(\frac{3}{2}, \frac{1}{2}, \frac{1}{2})$	4.736	3.679	-0.509
J_7	8 (↑)	$(1, 1, 1)$	5.319	1.763	0.3023

Fig. 3. Variation in the magnetic pair exchange parameters (in meV) as a function of volume for constant c/a ratio (=1.298). The equilibrium structure corresponds to $\Delta a/a_0$, where $a_0 = 2.73$ Å. The exchange parameters J_α are indexed by the crystallographic indices $J_{ij}(\vec{R})$. See Table 1.

to an overall FM instability in τ-$Mn_{0.54}Al_{0.46}$ under volume expansion.

To verify the predictions obtained from the above magnetic response calculations of $J_{\vec{R}}$ in τ-$Mn_{0.54}Al_{0.46}$, i.e., that the FM structure is unstable at expanded volumes, we computed the difference in the total energies of few AFM structures as a function of cell volumes. For a relative volume expansion of $\simeq 9\%$, with respect to the equilibrium, we find that the AFM-A and AFM-C structures are 59.32 and 16.08 meV/f.u lower in energy, in comparison with the FM ordering. The total energy of the AFM-G structure was 226.52 meV/f.u higher in energy. These findings evidence to increasing stability of AFM interactions in τ-$Mn_{0.54}Al_{0.46}$ via exchange inversion, thereby proving our predictions derived from the linear response calculations.

4. Summary and conclusion

In summary, our first-principles linear response calculations on rare-earth free permanent magnet τ-$Mn_{0.54}Al_{0.46}$ show competing FM and AFM Mn interactions. Such a co-existence of magnetic pair-exchanges between Mn ions in a system, with their interaction magnitudes being similar, usually points to a non-collinear magnetic structure. The finding is in contrast to the earlier assumption that τ-MnAl is a conventional type collinear FM system. Following these findings, we argue that non-collinear ordering of Mn magnetic moments in τ-MnAl is also a responsible factor in lowering the magnetization in τ-MnAl, as observed in the experiments, apart from the other factors such as formation of multiple phases and defects. Experimental corroboration of non-collinearity in τ-MnAl, with local probe experiments such as neutron diffraction, therefore require attention in understanding of the materials hard magnetic properties. The increase in magnetization, and thus the energy factor in τ-MnAl, with doping with non-magnetic components accomplished via addition of C and Zn [47–50], also seems to be linked with the modification of the equilibrium magnetic structure. The latter supposition, however, require further investigations in detail, both theoretically and experimentally.

Acknowledgments

References

[1] R.D. Heidenreich, E.A. Nesbitt, J. Appl. Phys. 23 (1952) 352.
[2] E.A. Nesbitt, R.D. Heidenreich, J. Appl. Phys. 23 (1952) 366.
[3] K. Yosida, M. Tachiki, Prog. Theor. Phys. 17 (1957) 331.
[4] F. Bolzoni, F. Leccabue, R. Panizzieri, L. Pareti, IEEE Trans. Magn. 20 (1984) 1625.
[5] T. Klemmer, D. Hoydick, H. Okumura, B. Zhang, W.A. Soffa, Scripta Met. Mater. 33 (1995) 1793.
[6] J.M.D. Coey, IEEE Trans. Magn.: Adv. Magn. 47 (2011) 4671.
[7] [2] J.B. Yang, K. Kamaraju, W.B. Yelon, W.J. James, Q. Cai, A. Bollero, Appl. Phys. Lett. 79 (2001) 1846.
[8] W.E. Stutius, T. Chen, T.R. Sandin, AIP Conf. Proc. 18 (1974) 1222.
[9] X. Guo, X. Chen, Z. Altounian, J. O Strom-Olsen, Phys. Rev. B 46 (1992) 14578.
[10] E. Adams, W.M. Hubbard, A.M. Syeles, J. Appl. Phys. 23 (1952) 1207.
[11] C. Chinnasamy, M.M. Jasinski, A. Ulmer, W. Li, G. Hadjipanayis, J. Liu, IEEE Trans. Magn. 48 (2012) 3641.
[12] C.L. Zha, R.K. Dumas, J.W. Lau, S.M. Mohseni, Sohrab R. Sani, I.V. Golosovsky, A.F. Monsen, J. Nogues, Johan Akerman, J. Appl. Phys. 110 (2011) 093902.
[13] H. Niida, T. Hori, H. Onodera, Y. Yamaguchi, Y. Nakagawa, J. Appl. Phys. 79 (1996) 5946.
[14] J. Winterlik, B. Balke, G.H. Fecher, C. Felser, M.C.M. Alves, F. Bernardi, J. Morais, Phys. Rev. B 77 (2008) 054406.
[15] T.J. Nummy, S. P Bennett, T. Cardinal, D. Heiman, Appl. Phys. Lett. 99 (2011) 252506.
[16] S. Mizukami, F. Wu, A. Sakuma, J. Walowski, D. Watanabe, T. Kubota, X. Zhang, H. Naganuma, M. Oogane, Y. Ando, T. Miyazaki, Phys. Rev. Lett. 106 (2011) 117201.
[17] H. Kono, J. Phys. Soc. Jpn. 13 (1958) 1444.
[18] Q. Zeng, I. Baker, Z.C. Yan, J. Appl. Phys. 99 (2006) 08E902.
[19] A.J.J. Koch, P. Hokkeling, M.G.v.d. Steeg, K.J. de Vos, J. Appl. Phys. 31 (1960) 75S.
[20] J.H. Park, Y.K. Hong, S. Bae, J.J. Lee, J. Jalli, G.S. Abo, N. Neveu, S.G. Kim, C.J. Choi, J.G. Lee, J. Appl. Phys. 107 (2010) 09A731.
[21] D.P. Hoydick, E.J. Palmiere, W.A. Soffa, J. Appl. Phys. 81 (1997) 5624.
[22] K. Kamino, T. Kawaguchi, M. Nagakura, IEEE Trans. Magn. 2 (1966) 506.
[23] Z.C. Yan, Y. Huang, Y. Zhang, G.C. Hadjipanayis, W. Soffa, D. Weller, Scr. Mater. 53 (2005) 463.
[24] A. Sakuma, J. Phys. Soc. Jpn. 63 (1994) 1422.
[25] P.B. Braun, J.A. Goedkoop, Acta Crystallogr. 16 (1963) 737.
[26] Y. Sakamoto, S. Kojima, T. Ohtani, T. Kubo, J. Appl. Phys. SO (1979) 2355.
[27] M.A. Bohlmann, J.C. Koo, J.H. Wise, J. Appl. Phys. 52 (1981) 2542.
[28] N.I. Vlasova, G.S. Kandaurova, VA.S. Shur, N.N. Bykhanova, Phys. Met. Metallorg. 51 (1981) 1.
[29] Y.J. Kim, J.H. Perepezko, Mater. Sci. Eng. A 163 (1993) 127.
[30] T.B. Massalski, Binary Alloy Phase Diagrams, TMS, Materials Park, 1990.
[31] A.J. McAlster, J.L. Murray, Binary Alloy Phase Diagrams, second ed., in: T.B. Massalski, P.R. Subramanian, H. Okamoto, and L. Kacprzak (Eds.), ASM Int. 171, 1990.
[32] J. Jensen, A.R. Mackintosh, Rare Earth Magnetism, Oxford University Press, Oxford, United Kingdom, 1991.
[33] I. Turek, V. Drchal, J. Kudrnovsky, M. Sob, P. Weinberger, Electronic Structure of Disordered Alloys, Surfaces and Interfaces, Kluwer Academic, Dordrecht, 1997.
[34] A.V. Ruban, H.L. Skriver, Comput. Mater. Sci. 15 (1999) 119.
[35] B.L. Gyorffy, A.J. Pindor, J.B. Staunton, G.M. Stocks, H. Winter, J. Phys. F: Met. Phys. 15 (1985) 1337.
[36] E.O. Wollan, W.C. Koehler, Phys. Rev. 100 (1955) 545563.
[37] Y. Kurtulus, R. Dronskowski, J. Solid State Chem. 176 (2003) 390.
[38] N.I. Vlasova, G.S. Kandaurova, Y.S. Shur, N.N. Bykhanova, Phys. Met. Metall. 51 (1981) 1.
[39] J.J. Wyslocki, A. Zygmunt, Acta Phys. Polon. A70 (1986) 29.
[40] W. Blau, C.H. Muller, H. Wonn, Phys. Status Solidi A59 (1980) K203.
[41] A.M. Bratkovsky, A.V. Smirnov, D.N. Manh, A. Pas- turel, Phys. Rev. B 52 (1995) 3056.
[42] A.V. Smirnov, A.M. Bratkovsky, Phys. Rev. B 53 (1996) 8515.
[43] A.I. Liechtenstein, M.I. Katsnelson, V.A. Gubanov, J. Phys. F: Met. Phys. 14 (1984) L125.
[44] A. I Liechtenstein, M.I. Katsnelson, V.P. Antropov, V.A. Gubanov, J. Magn. Magn. Mater. 67 (1987) 65.
[45] J. Kubler, Theory of Itinerant Magnetism Oxford Science Publications, Clarendon Press, Oxford, 2000.
[46] C. Herring, in: G. Rado, H. Suhl (Eds.), Magnetism IV, Academic Press, New York, 1966.
[47] T. Ohtani, N. Kato, S. Kojima, K. Kojima, Y. Sakamoto, I. Konno, M. Tsukahara, T. Kubo, IEEE Trans. Magn. 13 (1977) 1328.
[48] A.V. Dobromyslov, A.E. Ermakov, N.I. Taluts, M.A. Uimin, Phys. Status Solidi (a) 88 (1985) 443.
[49] Q. Zeng, I. Baker, J.B. Cui, Z.C. Yan, J. Magn. Magn. Mater. 308 (2007) 214.
[50] H.X. Wang, P.Z. Si, W. Jiang, J.G. Lee, C.J. Choi, J.J. Liu, Q. Wu, M. Zhong, H.L. Ge, Open J. Microphys. 1 (2011) 19.